INSTITUTE OF PHYSICS PUBLISHING JOURNAL OF PHYSICS: CONDENSED MATTER

J. Phys.: Condens. Matter **15** (2003) S1767–S1777 PII: S0953-8984(03)55593-X

DNA uptake into nuclei: numerical and analytical results

Zénó Farkas[1,2], **Imre Derényi**[1] **and Tamás Vicsek**[1]

[1] Department of Biological Physics, Eötvös University, Pázmány P Stny 1A, H-1117 Budapest, Hungary
[2] Department of Theoretical Physics, Gerhard-Mercator University, D-47048 Duisburg, Germany

E-mail: zeno@angel.elte.hu, derenyi@angel.elte.hu and vicsek@angel.elte.hu

Received 5 November 2002
Published 28 April 2003
Online at stacks.iop.org/JPhysCM/15/S1767

Abstract

The dynamics of polymer translocation through a pore has been the subject of recent theoretical and experimental works. We have considered theoretical estimates and performed computer simulations to understand the mechanism of DNA uptake into the cell nucleus, a phenomenon experimentally investigated by attaching a small bead to the free end of the double helix and pulling this bead with the help of an optical trap. The experiments show that the uptake is monotonic and slows down when the remaining DNA segment becomes very short. Numerical and analytical studies of the entropic repulsion between the DNA filament and the membrane wall suggest a new interpretation of the experimental observations. Our results indicate that the repulsion monotonically decreases as the uptake progresses. Thus, the DNA is pulled in either (i) by a small force of unknown origin, and then the slowing down can be interpreted only statistically, or (ii) by a strong but slow ratchet mechanism, which would naturally explain the observed monotonicity, but then the slowing down requires additional explanations. Only further experiments can unambiguously distinguish between these two mechanisms.

1. Introduction

In eukaryotic cells molecular transport between the nucleus and the cytoplasm takes place through the nuclear pore complexes (NPCs) [1, 2]. Ions and small proteins can diffuse through these large channels, but large proteins and protein–RNA complexes are transported actively via a signal-mediated process. DNA, on the other hand, is rarely transported under normal circumstances. However, this latter process might be relevant during viral infection or genetic therapy. In a recent elegant experiment the uptake of single DNA molecules into the nucleus was studied by the group of Elbaum [3]. In the present paper we provide a computational and theoretical study to understand and interpret the results of this experiment.

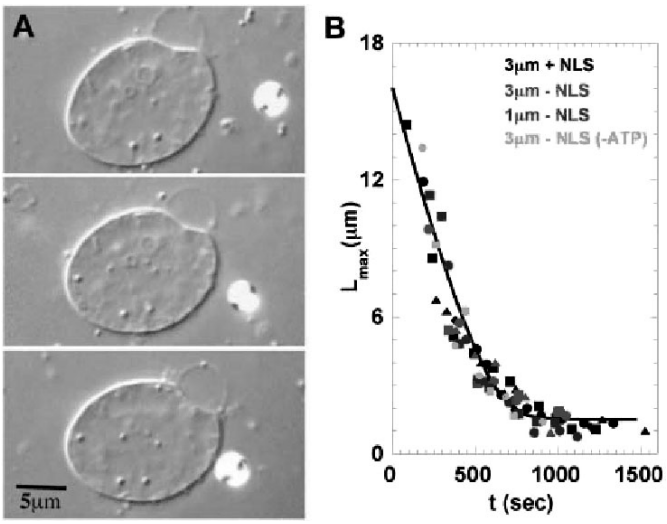

Figure 1. Kinetic measurement of DNA uptake. (A) The nucleus being dragged after a 3 μm diameter bead, linked by a DNA molecule. The time intervals between recording the images are 532 and 302 s, respectively. Note the shortening of the extended length of the DNA. (B) Measurements of the extended length versus time. The data were collected from many measurements. Since the initial moment of association between the DNA and the nuclear pore was unknown, all data were fitted to a common master curve (after [3]).

2. Description of the experiment

In the experiment double-stranded bacteriophage λ DNA was transported into cell-free nuclei of *Xenopus laevis* eggs. The DNA molecules were linked to polystyrene beads of 1 or 3 μm. Beads lying near a nucleus were trapped by optical tweezers and pulled away. In some cases dragging the bead pulled the whole nucleus behind it at a distance (figure 1(A)). After the bead was released, it started a biased Brownian motion due to thermal fluctuations and its attachment to the DNA segment. Such stretches were repeated on the same bead at 2 min intervals, and the maximum extension decreased with each measurement (figure 1(B)). This suggests that some mechanism inside the nucleus pulled the DNA inward. The remaining extended length versus time curve has two main features: (i) it starts linearly, and (ii) the length does not go to zero; instead, it converges to about 1 μm. The uptake itself is very slow (compared to the timescale of biochemical processes in living organisms); it takes several hundred seconds for a 10 μm long DNA.

3. Theoretical estimates for the entropic forces

To explain the convergence of the remaining length versus time curve and to give some estimations for the *uptake force* and the *effective friction coefficient* of the pore, Salman *et al* [3] proposed a model in which the shrinking remaining segment of the DNA applies an *increasing* resistance against the uptake. They argue that because the entropic spring constant of a chain of length L is proportional to L^{-1} and the average separation of the two ends of the remaining DNA segment (caused by volume exclusion by the bead and the nucleus) is proportional to $L^{1/2}$, the resulting entropic repulsion diverges as their product, $L^{-1/2}$.

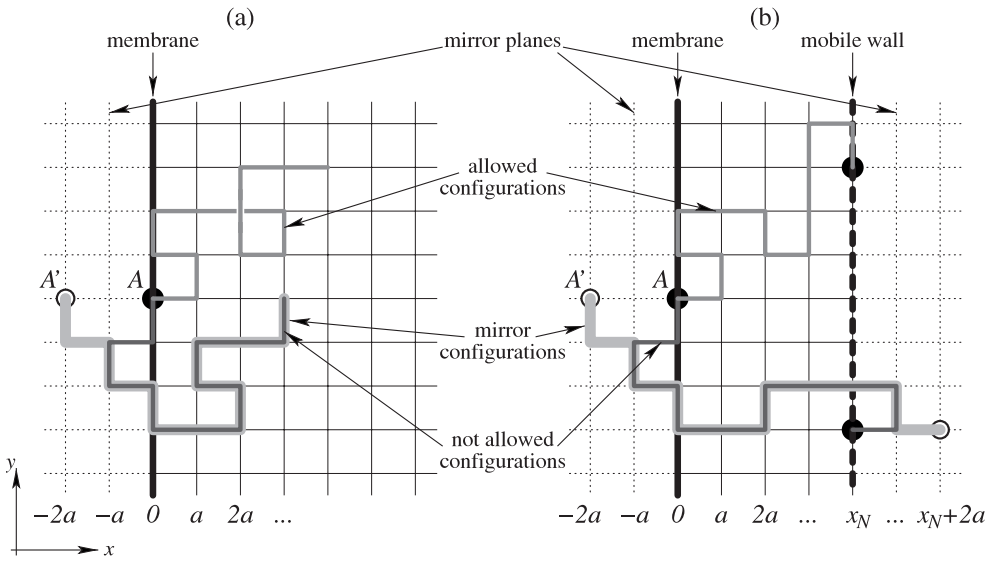

Figure 2. Lattice chains of length $L = 13a$, depicted in 2D. One end of the chains is anchored to the membrane at point A, while the other end is either (a) free, or (b) bound to a mobile wall. The figures indicate how to construct the mirror configuration (light grey curves) of a configuration not allowed by the constraints (dark grey curves).

However, a detailed statistical analysis (described below) shows the opposite: the entropic repulsion imposed by the shrinking DNA segment *decreases* as $-L^{-1}$. This result makes it necessary to reconsider the proposed kinetics of the uptake of DNA by the nucleus.

It has long been known that a polymer of length L, anchored at one of its ends to a wall (with the other end being free), pulls on the wall with the force

$$F_{\text{free ended}} = F^{\infty}_{\text{free ended}} - (1-\gamma)\frac{k_{\text{B}}T}{L} \tag{1}$$

at the anchoring point, on average [4–6]. T denotes the absolute temperature, k_{B} is the Boltzmann constant and the length independent force term $F^{\infty}_{\text{free ended}} > 0$ depends on the means of anchoring and on other properties of the polymer. $\gamma \approx 0.69$ for self-avoiding and $\gamma = 1/2$ for non-self-avoiding polymers. Due to force balance the rest of the polymer pushes the wall with the same amount of force.

Below we show that for non-self-avoiding polymers equation (1) can be obtained in a way much simpler than the original derivation, using a simple *lattice chain* model. Then we develop further this approach to take into account the role of the bead.

If the *persistence length* of the polymer is L_{p}, the lattice constant of the equivalent three-dimensional lattice chain is $a = 2L_{\text{p}}$, which is called the *Kuhn length* [7]. Let us suppose that the wall is located at the $x = 0$ plane, and the anchoring point is at the origin A $= (0, 0, 0)$, as depicted in figure 2. The constraint that the chain is not allowed to pierce through the wall is modelled by the condition that none of the x coordinates of the chain points can be negative: $0 \leqslant x_i$, where $0 \leqslant i \leqslant N$ and $N = L/a$ is the number of Kuhn segments. The partition function $\mathcal{Z}$ of this system is simply the sum of all possible chain configurations that satisfy the above condition.

Let us choose an arbitrary point B in the $0 \leqslant x$ half-space. According to the so-called *reflection principle*, each configuration that connects A and B but does not satisfy the constraint

has one and only one 'mirror configuration' that connects $A' = (-2a, 0, 0)$ and B. Illustrated in figure 2(a), the mirror configuration is obtained by reflecting every chain point from A to the first unsatisfied point about the $x = -a$ plane. Denoting the number of unconstrained configurations that connect points P and Q by $\mathcal{N}(\mathrm{P} \rightarrow \mathrm{Q})$, the partition function can be expressed as

$$\mathcal{Z} = \sum_{x_N \geqslant 0, y_N, z_N} \{\mathcal{N}[\mathrm{A} \rightarrow (x_N, y_N, z_N)] - \mathcal{N}[\mathrm{A}' \rightarrow (x_N, y_N, z_N)]\}, \tag{2}$$

where each configuration that is counted mistakenly in the first term is cancelled by its mirror configuration in the second term. The partition function can further be written as

$$\begin{aligned}\mathcal{Z} &= \sum_{x_N \geqslant 0, y_N, z_N} \{\mathcal{N}[\mathrm{A} \rightarrow (x_N, y_N, z_N)] - \mathcal{N}[\mathrm{A} \rightarrow (x_N + 2a, y_N, z_N)]\} \\ &= \sum_{x_N \in \{0,a\}, y_N, z_N} \mathcal{N}[\mathrm{A} \rightarrow (x_N, y_N, z_N)] \\ &\approx (2d)^N \mathcal{P}(0 \leqslant x_N < 2a) \approx (2d)^N 2a\rho(0),\end{aligned} \tag{3}$$

where $d = 3$ is the dimension of the space, $\mathcal{P}(0 \leqslant x_N < 2a)$ is the probability that the chain ends between the planes $x = 0$ and $2a$ in the continuum limit and $\rho(x) = (2\pi\sigma^2)^{-1/2} \exp[-x^2/(2\sigma^2)]$ is the probability density of the x coordinate of the end position with $\sigma^2 = a^2 N/d$. The approximations are valid for large N.

Thus, the partition function can be expressed as

$$\mathcal{Z} \approx \pi^{-1/2} (2d)^N \left(\frac{2d}{N}\right)^{1/2}, \tag{4}$$

the free energy is

$$\mathcal{F} = -k_\mathrm{B} T \ln(\mathcal{Z}) \tag{5}$$

and the force acting on the anchored end of the chain is

$$F_{\text{free ended}} = -\frac{\partial \mathcal{F}}{\partial L} = -\frac{1}{a}\frac{\partial \mathcal{F}}{\partial N} \approx k_\mathrm{B} T \frac{\ln(2d)}{2L_\mathrm{p}} - \frac{1}{2}\frac{k_\mathrm{B} T}{L}, \tag{6}$$

in agreement with equation (1).

In the experiments, however, the distal end of the polymer is not free, but is bound to a polystyrene bead. Because the bead is large compared to the remaining DNA coil when the uptake stalls, we can approximate it with a mobile wall. The lattice chain calculation can be repeated even for this system. The partition function, i.e., the number of allowed configurations, is now

$$\begin{aligned}\mathcal{Z} = \sum_{x_N \geqslant 0, y_N, z_N} &\{\mathcal{N}[\mathrm{A} \rightarrow (x_N, y_N, z_N)] - \mathcal{N}[\mathrm{A}' \rightarrow (x_N, y_N, z_N)] \\ &- \mathcal{N}[\mathrm{A} \rightarrow (x_N + 2a, y_N, z_N)] + \mathcal{N}[\mathrm{A}' \rightarrow (x_N + 2a, y_N, z_N)]\},\end{aligned} \tag{7}$$

where the first two terms are from equation (2), the third term—based on the reflection principle again (see figure 2(b))—cancels all configurations that go beyond the end point (x_N, y_N, z_N) and the fourth term compensates for those configurations that have been cancelled twice (in both the second and the third terms). Replacing $\mathcal{N}[\mathrm{A}' \rightarrow (x_N, y_N, z_N)]$ by $\mathcal{N}[\mathrm{A} \rightarrow (x_N + 2a, y_N, z_N)]$ and $\mathcal{N}[\mathrm{A}' \rightarrow (x_N + 2a, y_N, z_N)]$ by $\mathcal{N}[\mathrm{A} \rightarrow (x_N + 4a, y_N, z_N)]$ and making further simplifications one arrives at

$$\begin{aligned}\mathcal{Z} &= \sum_{x_N \in \{0,a\}, y_N, z_N} \mathcal{N}[\mathrm{A} \rightarrow (x_N, y_N, z_N)] - \sum_{x_N \in \{2a,3a\}, y_N, z_N} \mathcal{N}[\mathrm{A} \rightarrow (x_N, y_N, z_N)] \\ &\approx (2d)^N 2a[\rho(0) - \rho(2a)] \approx \pi^{-1/2} (2d)^N \left(\frac{2d}{N}\right)^{3/2},\end{aligned} \tag{8}$$

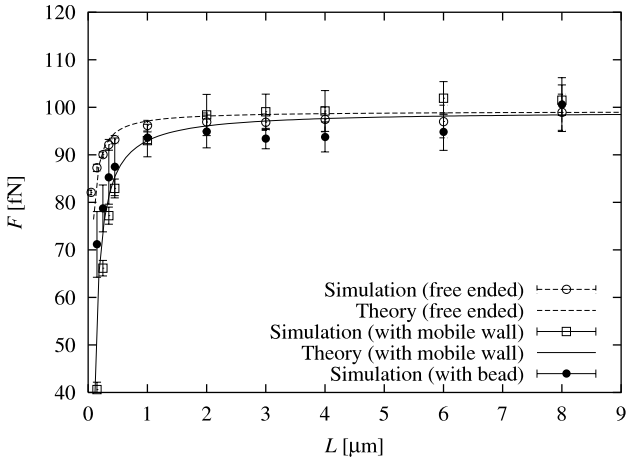

Figure 3. The force exerted by the membrane as a function of the polymer length. The symbols are the results of numerical simulations with $b = 50$ nm, averaged over ten 2 s long runs. The curves are theoretical predictions (shifted upward to fit the data set).

leading to the entropic force

$$F_{\text{mobile wall}} \approx k_{\text{B}}T\frac{\ln(2d)}{2L_{\text{p}}} - \frac{3}{2}\frac{k_{\text{B}}T}{L}, \tag{9}$$

which indicates that a bead (or mobile wall) attached to the end of the DNA renders the entropic resistance even smaller. This can be understood intuitively by noticing that near the end of the uptake process the geometric constraints drastically reduce the available configuration space for the remaining segment, so it becomes more and more favourable for the DNA to slide through to the other side of the membrane.

Although the reflection principle can only be applied to non-self-avoiding polymers, we expect a qualitatively similar behaviour for self-avoiding ones, too. In this latter case the reduction of the configuration space should also decrease the entropic resistance.

To verify our theoretical estimations we have performed numerical simulations. As figure 3 indicates, the numerical results for the free ended filament and for the one with the mobile wall are in good agreement with the relevant terms $-k_{\text{B}}T/(2L)$ and $-3k_{\text{B}}T/(2L)$ of the theoretical predictions, respectively. The case with the polystyrene bead, just as expected, is in between the above two extremes, closer to the one with the mobile wall.

4. Simulation technique

We modelled the double-stranded DNA as a three-dimensional 'bead–rod' chain [7], and used molecular dynamics simulations to follow its dynamics (see figure 4). Note that the 'beads' of the bead–rod chain are artificial units and have nothing to do with the polystyrene bead in the real experiment. Monte Carlo methods were ruled out because they usually fail to reproduce the correct dynamics.

The overdamped equations of motion of the beads are

$$\Gamma\dot{\boldsymbol{R}}_j = \boldsymbol{F}_j^{\text{constr}} + \boldsymbol{F}_j^{\text{bend}} + \boldsymbol{F}_j^{\text{metr}} + \boldsymbol{F}_j^{\text{ext}} + \boldsymbol{\xi}_j, \tag{10}$$

where Γ is the friction coefficient and $\boldsymbol{R}_j$ is the position of the jth bead ($1 \leqslant j \leqslant N+1$). The bond vectors can be defined as $\boldsymbol{r}_j = \boldsymbol{R}_{j+1} - \boldsymbol{R}_j$ (for $1 \leqslant j \leqslant N$). The forces on the rhs of the equations are as follows.

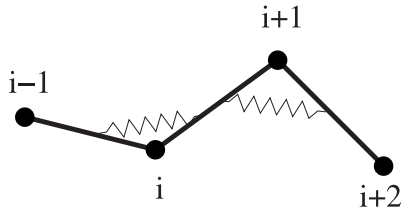

Figure 4. Discretized polymer: the beads are connected by the rigid rods (bonds), and the bending elasticity is taken into account by angular springs.

- $\boldsymbol{F}_j^{\mathrm{constr}}$ is the constraint force. These forces are responsible for keeping the length of the rods (or bonds) fixed: $|\boldsymbol{r}_j| = b$. The constraint forces can be decomposed into the bond tension forces: $\boldsymbol{F}_j^{\mathrm{constr}} = \boldsymbol{F}_j^{\mathrm{tens}} - \boldsymbol{F}_{j-1}^{\mathrm{tens}}$ with $\boldsymbol{F}_j^{\mathrm{tens}} = T_j \boldsymbol{r}_j$ and $\boldsymbol{F}_0^{\mathrm{tens}} = \boldsymbol{F}_{N+1}^{\mathrm{tens}} = 0$ [9]. The tensions T_j represent N new variables; however, we have exactly this number of additional equations expressing that the bond lengths are constant: $\boldsymbol{r}_j \cdot \dot{\boldsymbol{r}}_j = 0$.
- $\boldsymbol{F}_j^{\mathrm{bend}}$ is the bending force. The bending resistance is represented by angular springs between the adjacent bonds. The bending energy is $E^{\mathrm{bend}} = \frac{\kappa(b)}{2b} \sum_{i=1}^{N-1} \theta_i^2$, where $\kappa(b)$ is the *bond length dependent* bending modulus, $\theta_i = \arccos(\boldsymbol{r}_i \cdot \boldsymbol{r}_{i+1}/b^2)$ is the included angle between bonds i and $i+1$. The bending force is thus $\boldsymbol{F}_j^{\mathrm{bend}} = -\nabla_j E^{\mathrm{bend}}$. In the literature the bending modulus of the continuous polymer, κ_0, is usually used to calculate the bending energy even in a discretized polymer model. However, for a discretized bead–rod polymer the bending modulus should depend on the bond length to give the correct statistics [8]. For example, one would expect that for $b = 2L_{\mathrm{p}}$ the bending modulus disappears, recovering the freely jointed chain model. A good approximation for the discretized bending modulus is $\hat{\kappa}(\hat{b}) \approx 1 - \hat{b}/6 + \hat{b}^2(4/\pi^2 - 13/24) + \hat{b}^3(1/6 - 2/\pi^2) + \hat{b}^4/96$, where $\hat{b} = b/L_{\mathrm{p}}$ is the dimensionless bond length and $\hat{\kappa}(\hat{b}) = \kappa(b)/\kappa_0$ is the dimensionless bending modulus. The persistence length L_{p} of the polymer is related to the bending modulus through the expression $L_{\mathrm{p}} = \kappa_0/(k_{\mathrm{B}}T)$. As expected, for $b \to 0$, $\kappa(b) \to \kappa_0$, and for $b = 2L_{\mathrm{p}}$, $\kappa(b) = 0$.
- $\boldsymbol{F}_j^{\mathrm{metr}}$ is the *metric* or *pseudo* force, and is needed because the motion of a bead–rod chain in a thermal bath is different from the limiting case of very stiff bonds [10–14]. The latter is a better model for real biopolymers, and the metric force turns the rigid rods into very stiff springs. $\boldsymbol{F}_j^{\mathrm{metr}} = -k_{\mathrm{B}}T \nabla_j \ln \sqrt{|g|}$, where g is the metric tensor of the hypersurface of the constrained $N+1$ beads in the originally $3(N+1)$-dimensional configuration space. The explicit form of this metric tensor for a linear bead–rod chain can be found in [10, 14].
- $\boldsymbol{F}_j^{\mathrm{ext}}$ is an optional external force acting on bead j. In the application presented in this paper, the polystyrene bead is attached to the end of the polymer by applying an attracting external force on the last polymer bead, while this bead and the wall of the nucleus exert repelling forces on the polymer. In certain situations the bond length b might be too large compared to the size of the surrounding objects. For example, in our simulation the DNA molecule goes through a 10 nm wide pore embedded in a 100 nm thick membrane wall, while the bond length is $b = 100$ nm. Because the DNA inside this narrow pore is almost straight, it is not necessary to choose a finer discretization of the chain; however, the forces should be monitored at a higher resolution. For this reason we introduced M 'virtual' beads along each rod, spaced uniformly. Their sole role is that external forces can act on them, and they appropriately redistribute these forces to the original beads at both ends of the bond they are sitting on. Hence, their presence improves the spatial resolution, as far as the external forces are concerned. We used $M = 10$ in the simulations.

- $\boldsymbol{\xi}_j$ represents spatially and temporally uncorrelated thermal noise, obeying the fluctuation–dissipation relation $\langle \boldsymbol{\xi}_j(t)\boldsymbol{\xi}_k(t')\rangle = 6k_{\mathrm{B}}T\Gamma\delta_{jk}\delta(t-t')$.

In our model we neglected the excluded volume effect for the DNA filament itself, although we accounted for the exclusion of the filament by the polystyrene bead and the nuclear membrane wall. Hydrodynamic interactions were also neglected.

In our simulations the persistence length was $L_{\mathrm{p}} = 50$ nm and the friction coefficient of the beads was $\Gamma \approx \pi\eta b$, where the viscosity of the water is $\eta = 10^{-3}$ kg s^{-1} m^{-1} and the temperature is $T = 300$ K. We used the second-order Runge–Kutta (or midpoint) method to solve the system of first-order ordinary equations [15]. The bond length b varied between 50 and 100 nm.

One can rely on the results of a dynamical simulation only if it is numerically stable. Therefore, it is important to be aware of the physical processes that determine the largest possible time step. In our case the diffusion of the polymer beads and the relaxation of the angular springs pose an upper limit for the time step. The typical distance a diffusive particle takes during time Δt is $\Delta x = \sqrt{2D\Delta t}$, where the diffusion constant is $D = k_{\mathrm{B}}T/\Gamma$. To ensure that the typical change of the bond length is smaller than a small fraction $\varepsilon_D b$ of the bond length, the time step cannot be larger than

$$\Delta t_D = \frac{\tilde{\Gamma}\varepsilon_D^2}{2k_{\mathrm{B}}T}b^3,$$

where $\tilde{\Gamma} = \Gamma/b$ is the friction coefficient per unit length. Here the constraint forces were not taken into account. However, we expect that even with the constraint forces in effect the numerical error is still proportional to the typical diffusive displacement of the beads in one time step.

The relaxation time of the angular springs is [16]

$$\tau_{AS} = \frac{\tilde{\Gamma}}{6\kappa(b)}b^4.$$

Apart from the prefactor, this can be easily seen from dimensional analysis. Thus, the time step cannot be larger than $\Delta t_{AS} = \varepsilon_{AS}\tau_{AS}$ either, where $\varepsilon_{AS} \ll 1$. In our simulations we used $\varepsilon_D = \varepsilon_{AS} = 0.05$. The maximum allowable time step is then the minimum of Δt_D and Δt_{AS}.

5. Discussion

A DNA filament threading through a nuclear pore is pulled by two opposing entropic forces from the two sides of the membrane. If the media on the two sides are identical, the length independent force terms cancel each other. Because the length dependent contributions (being proportional to $k_{\mathrm{B}}T/L$) disappear quickly for large L, there must exist some active (energy consuming) mechanism responsible for the pulling of the DNA. Since the integral of the length dependent term (from L_{p} to the total length of the DNA) is of the order of only a few $k_{\mathrm{B}}T$, this force term is not even strong enough to trap the DNA in a configuration where almost the entire DNA molecule is on one side of the membrane.

5.1. Chemical composition difference

The simplest way to implement an active pulling mechanism is to produce a difference between the length independent terms of the entropic forces on the two sides of the membrane. This can be achieved, e.g., via a difference in the ionic strengths or the pH values of the two media. Even the simple lattice chain model can account for this effect if the chemical composition of the medium affects the persistence length L_{p} of the DNA (see equations (6) and (9)).

5.2. Ratchet mechanism

Another possibility for the pulling is based on a ratchet mechanism [17]. The ratchet mechanism as a means of active transport was first proposed by the group of Oster [18, 19]. The idea is that inside the nucleus some kind of molecule is able to bind to the DNA with a rate constant k_{on} and to detach from it with a rate constant k_{off}. When such a molecule is bound to the DNA at some location, the DNA cannot slide back beyond this point.

Assuming that the possible binding sites for the molecule are separated by a distance b, we can estimate the effective pulling force produced by this ratchet mechanism. The grand canonical partition function per binding site is $\mathcal{Z} = 1 + \mathrm{e}^{-(E_b-\mu)/(k_{\mathrm{B}}T)}$, where E_b is the binding energy and μ is the chemical potential for the molecule. The probability that the site is unoccupied is $p_{\mathrm{off}} = 1/\mathcal{Z}$, and the probability that it is occupied is $p_{\mathrm{on}} = \mathrm{e}^{-(E_b-\mu)/(k_{\mathrm{B}}T)}/\mathcal{Z}$. Thus, the partition function can be written as $\mathcal{Z} = 1 + p_{\mathrm{on}}/p_{\mathrm{off}} = 1 + k_{\mathrm{on}}/k_{\mathrm{off}}$. The free energies of a binding site inside and outside the nucleus are $\mathcal{F}_{\mathrm{in}} = -k_{\mathrm{B}}T \ln \mathcal{Z}$ and $\mathcal{F}_{\mathrm{out}} = -k_{\mathrm{B}}T \ln 1 = 0$, respectively. Finally, an effective pulling force can be defined as

$$F_{\mathrm{ratchet}} = -(\mathcal{F}_{\mathrm{in}} - \mathcal{F}_{\mathrm{out}})/b = \ln\bigl(1 + k_{\mathrm{on}}/k_{\mathrm{off}}\bigr)k_{\mathrm{B}}T/b. \tag{11}$$

Note that this is the force necessary to stop the pulling. The pulling speed is proportional to this effective force only if the equilibration time of the binding of the molecules $(k_{\mathrm{on}} + k_{\mathrm{off}})^{-1}$ is shorter than the diffusion time of the DNA over the distance b. Otherwise the pulling speed is smaller.

5.3. Friction in the pore

The friction of the DNA inside the nuclear pores can significantly slow down the uptake process. Let us just estimate how long it would take for an entire DNA molecule to diffuse through the pore if there were no friction inside. As long as the pore is shorter than the Kuhn length (which is the case in our system), the diffusion can be envisioned as the subsequent diffusion of $N = L_{\mathrm{DNA}}/a$ Kuhn segments (where $a = 2L_{\mathrm{p}}$ is the Kuhn length). The diffusion time of a Kuhn segment can be approximated as $\tau_{\mathrm{K}} = (1/2)a^2(\pi\eta a)/(k_{\mathrm{B}}T)$, thus the diffusion time of the entire DNA molecule is about $\tau = N^2\tau_{\mathrm{K}} = L_{\mathrm{DNA}}^2 L_{\mathrm{p}}(\pi\eta)/(k_{\mathrm{B}}T)$. As expected for a polymer without self-exclusion, the diffusion time is proportional to the square of its length [20].

The diffusion time τ for a 15 μm long DNA molecule is in the order of 10 s. Because the uptake occurs much more slowly, in the order of 1000 s, the friction in the pore must be at least 100-fold greater than the hydrodynamic friction: $\Gamma_{\mathrm{pore}} > 100 L_{\mathrm{p}}\pi\eta \approx 10^{-8}$ kg s^{-1}. Such a strong friction can be explained by weak binding of the DNA to the nuclear pore [21].

5.4. Uptake kinetics I: weak pulling

The experiments show that the uptake slows down in the end and the remaining length of the DNA converges to $L_{\mathrm{conv}} \approx 1$ μm. A constant pulling force F (produced by either a chemical composition difference or a ratchet mechanism) corresponds to a linear potential $U(L) = FL$ with a reflecting boundary at $L = 0$. In such a potential the expectation value of L at equilibrium is given by $k_{\mathrm{B}}T/F$. Thus, the measured equilibrium distance L_{conv} is compatible with an $F = k_{\mathrm{B}}T/L_{\mathrm{conv}} \approx 4$ fN pulling force. From the average pulling speed, $v \approx 2 \times 10^{-8}$ m s^{-1}, one can also calculate the friction coefficient: $\Gamma_{\mathrm{pore}} = F/v \approx 2 \times 10^{-7}$ kg s^{-1}, which satisfies the condition given in the preceding paragraph.

It would result in an even smaller pulling force and friction coefficient if the length dependent term of the entropic force were also taken into account in the calculation of the equilibrium distance.

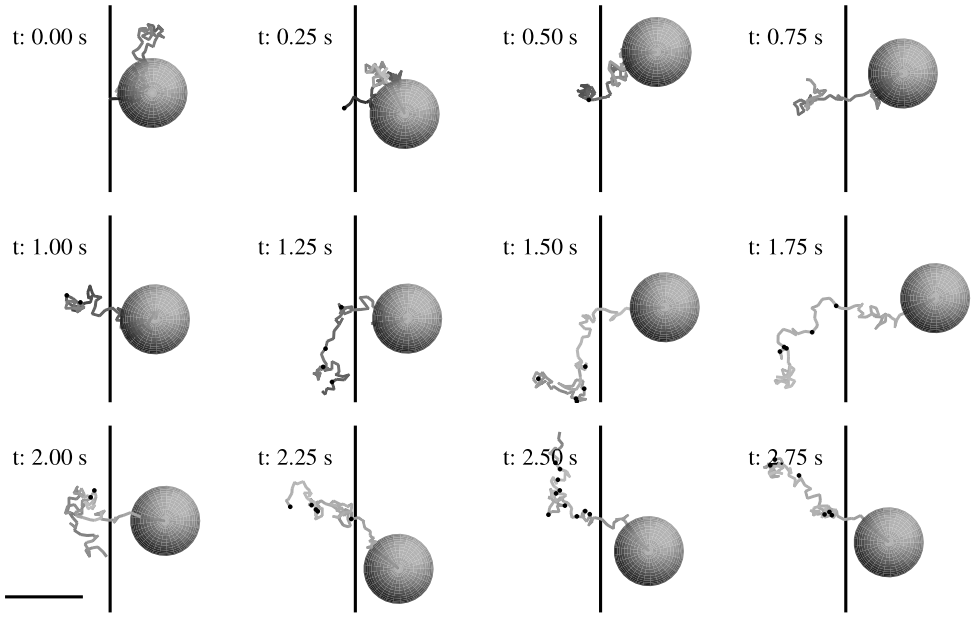

Figure 5. The uptake of a DNA filament. Its length is 8 μm, the bond length is $b = 100$ nm and the radius of the polystyrene bead is $R_b = 500$ nm. The black dots represent occupied binding sites. The horizontal bar in the bottom left corner corresponds to 1 μm. The grey scale indicates the position in the third dimension (depth).

We studied the uptake process by the ratchet mechanism using numerical simulations. We assumed that the molecules could bind only to the beads of the bead–rod chain. The simulations started from a configuration in which one end of the DNA had already got through the pore, and the first bead was not allowed to slip back through the pore. To mimic the experiment, a large bead of radius R_b was attached to the other, outer end of the DNA. The diameter of the pore was 10 nm, the width of the wall was 100 nm and the friction at the pore was neglected. Figure 5 shows a sequence of such a simulation.

Identifying the extended length of the remaining DNA by its arc length, in figure 6 we plotted the extended length versus time curve, averaged over 20 runs. It resembles the experimental curve: it starts linearly and converges to a constant value, about 1 μm, which coincides with the experimental one. The timescale of the simulation is shorter than that of the experiments, because we omitted the friction inside the pore, in order to save computational time.

The negative side of this interpretation is that the uptake is stochastic. Individual runs show back-slips at both the linear and the horizontal parts of the curve. The stationary state of the system is not an energy minimum but a dynamic equilibrium between the fluctuations of the DNA filament and the weak pulling of the transport mechanism. Since such fluctuations are not apparent in the experiments, we examine another possibility for the kinetics of the uptake.

5.5. Uptake kinetics II: strong but slow ratcheting

A monotonic uptake can be achieved either by a strong continuous pulling in conjunction with a strong friction or by a strong but slow ratchet mechanism. In such a ratchet mechanism the speed of the uptake would be set by the small binding rate k_{on}, and the even much smaller unbinding

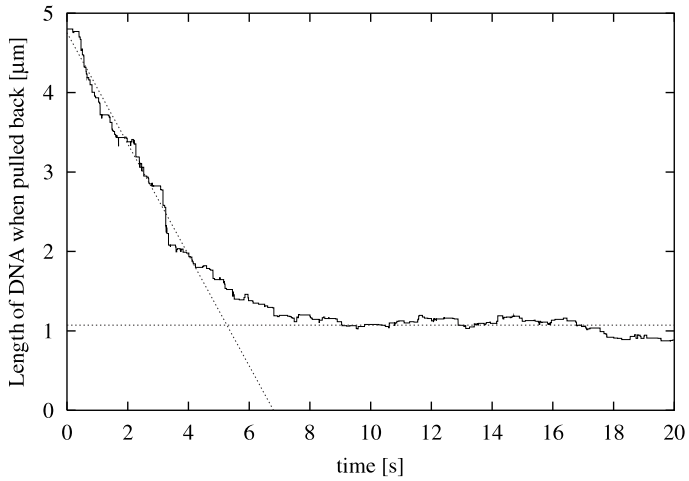

Figure 6. The remaining length of the DNA versus time curve. The parameters are $k_{\rm on} = 0.1\ {\rm s}^{-1}$, $k_{\rm off} = 0.25\ {\rm s}^{-1}$, $b = 100$ nm, $R_{\rm b} = 0.2\ \mu$m and the total length of the DNA is 4.8 μm. The curve is an average over 20 runs.

rate $k_{\rm off} \ll k_{\rm on}$ would ensure that unbinding is negligibly rare and, thus, the ratcheting is practically irreversible. Note that although the large $k_{\rm on}/k_{\rm off}$ ratio corresponds to a large effective (equilibrium) pulling force, it is not manifested in the speed of the uptake (which is a non-equilibrium process).

Due to the negligibly rare unbinding events the ratchet mechanism is also supported by the fact that the uptake can be stopped but never reversed in the experiments [3] by applying picoNewton forces on the polystyrene bead. A continuous pulling would be incompatible with this observation.

The only phenomenon that cannot be explained by such a ratchet mechanism is the convergence of the remaining length to a non-zero value. There are, however, alternative explanations for this:

- the non-zero distance might be an artifact of the image processing;
- there might be unknown structures on the nuclear envelope that prevent the polystyrene bead from getting in contact with the nucleus;
- the picoNewton forces used to extend the DNA might be sufficiently strong to deform the membrane by hundreds of nanometres at the vicinity of the pore [22, 23];

or a combination of these.

6. Conclusions

Our numerical and analytical studies of the uptake of DNA filaments into the nucleus suggest two possible mechanisms for the uptake process. None of them can be ruled out on the basis of existing experimental data. One of the mechanisms explains the convergence of the remaining length of the DNA to a finite value, but has an intrinsically stochastic nature (back-slips occur). This mechanism alone cannot account for the stopping of the uptake under retarding forces in the picoNewton range. The other mechanism seems more plausible: it predicts a monotonic uptake, but requires additional elements to explain the convergence. Only further experiments can unambiguously distinguish between these mechanisms, focusing on their differences.

Acknowledgments

We would like to acknowledge Collegium Budapest for its hospitality. We also thank M Elbaum for many useful discussions and helpful comments. This research has been supported by the Hungarian National Research Grant Foundation (OTKA T033104).

References

[1] Elbaum M 2001 The nuclear pore complex: biochemical machine or Maxwell demon? *C. R. Acad. Sci., Paris* IV **2** 861–70
[2] Alberts B *et al* 2002 *Molecular Biology of the Cell* 4th edn (New York: Garland)
[3] Salman H, Zbaida D, Rabin Y, Chatenay D and Elbaum M 2001 Kinetics and mechanism of DNA uptake into the cell nucleus *Proc. Natl Acad. Sci. USA* **98** 7247–52
[4] Eisenriegler E 1993 *Polymers Near Surfaces* (Singapore: World Scientific)
[5] Sung W and Park P J 1996 Polymer translocation through a pore in a membrane *Phys. Rev. Lett.* **77** 783–6
[6] Muthukumar M 1999 Polymer translocation through a hole *J. Chem. Phys.* **111** 10371–4
[7] Doi M and Edwards S F 1986 *The Theory of Polymer Dynamics* (Oxford: Clarendon)
[8] Frank-Kamenetskii M D, Lukashin A V, Anshelevich V V and Vologodskii A V 1985 Torsional and bending rigidity of the double helix from data on small DNA rings *J. Biomol. Struct. Dyn.* **2** 1005–12
[9] Everaers R, Jülicher F, Ajdari A and Maggs A C 1999 Fluctuations of semiflexible filaments *Phys. Rev. Lett.* **82** 3717–20
[10] Fixman M 1974 Classical statistical mechanics of constraints: a theorem and applications to polymers *Proc. Natl Acad. Sci. USA* **74** 3050–3
[11] Fixman M 1978 Simulation of polymer dynamics: I. General theory *J. Chem. Phys.* **69** 1527–37
[12] Hinch E J 1994 Brownian motion with stiff bonds and rigid constraints *J. Fluid Mech.* **271** 219–34
[13] Grassia P S, Hinch E J and Nitsche L C 1995 Computer simulations of Brownian motion of complex systems *J. Fluid. Mech.* **282** 373–403
[14] Grassia P and Hinch E J 1996 Computer simulations of polymer chain relaxation via Brownian motion *J. Fluid. Mech.* **308** 255–88
[15] Press W H, Teukolsky S A, Vetterling W T and Flannery B P 1992 *Numerical Recipes in C* (Cambridge: Cambridge University Press)
[16] Farkas Z 2001 Transport by ratchet mechanism: application to granules and DNA *PhD Thesis* Eötvös University, Budapest
[17] Elbaum M 2001 private communication
[18] Simon S M, Peskin C S and Oster G F 1992 What drives the translocation of proteins? *Proc. Natl Acad. Sci. USA* **89** 3770–4
[19] Peskin C S, Odell G M and Oster G F 1993 Cellular motions and thermal fluctuations: the Brownian ratchet *Biophys. J.* **65** 316–24
[20] Chuang J, Kantor Y and Kardar M 2001 Anomalous dynamics of translocation *Phys. Rev.* E **65** 011802
[21] Lubensky D K and Nelson D R 1999 Driven polymer translocation through a narrow pore *Biophys. J.* **77** 1824–38
[22] Derényi I, Jülicher F and Prost J 2002 Formation and interaction of membrane tubes *Phys. Rev. Lett.* **88** 238101
[23] Powers T R, Huber G and Goldstein R E 2002 Fluid–membrane tethers: minimal surfaces and elastic boundary layers *Phys. Rev.* E **65** 041901